10th International IFAC Symposium on
Computer Applications in Biotechnology
Preprints Vol.1, June 4-6, 2007, Cancún, Mexico

MODEL FORMULATION FOR HYBRIDOMA CULTURES IN BATCH AND FED-BATCH MODE

Penny Dorka, Christian Fischer*, Hector M. Budman[1], Jeno M. Scharer

Dept Chemical Engineering, University of Waterloo, Waterloo, ON, Canada, N2L3G1
** Technical University of Braunschweig, Braunschweig, Germany*

Abstract: Metabolic Flux Analysis was performed to identify the significant metabolic reactions for hybridoma cells during batch and fed-batch culture. Correlation analysis yielded the factors that influence biomass growth and productivity and elucidated the nature of the relationship between them. Consequently, an integrated dynamic model expressing the rate of consumption and production of nutrients/metabolites and the biomass growth and decline was developed.

Keywords: hybridoma, metabolic flux, quadratic programming, cross-correlation functions, parameter-estimation, prediction.

1. INTRODUCTION

The large-scale production of monoclonal antibodies (MAb) by mammalian cells in batch and fed-batch culture systems is limited by the unwanted decline in cell viability and reduced productivity that may result from changes in culture conditions. Therefore, it becomes imperative to gain an in-depth knowledge of the factors affecting cell viability and subsequently antibody production. The aim of the present work is to obtain an overall dynamic model that predicts the behaviour of both batch and fed-batch systems as a function of the extra-cellular nutrient/metabolite concentration at any time and utilize this model for optimization of Monoclonal antibody (MAb) production in the future.

Although considerable effort has been made to understand the kinetics of hybridoma growth and metabolism, it has become evident that a model structure is not a priori obvious. A systematic approach based on Metabolic Flux Analysis (MFA) has been proposed by Provost and Bastin (2004) and applied by Gao, *et al.*, (2006) with some modifications for batch production of MAb. MFA permits to calculate values of intracellular fluxes from available extracellular fluxes, some of which are significant and some are negligible. Thus, the original metabolic network can be reduced to contain only the reactions corresponding to the significant fluxes that are then used to formulate a set of fundamental macro- reactions linking the substrates to the products, thus eliminating involvement of intracellular metabolite concentrations in the mathematical model. A set of dynamic mass balances can be devised that involve rate expressions for the consumption/production of substrates/ metabolites.

In previous studies, the MFA analysis has been done for batch operations (Provost and Bastin, 2004). Also, in the development of the MFA and the resulting dynamic model for metabolites, the viable and dead cell concentrations and their corresponding rates of change have not been explicitly modeled. Instead, their experimental values have been used as an input for the metabolites model.

The current work addresses these issues as follows:

1. MFA is applied to a fed batch situation in order to obtain a dynamic model for this

[1]Corresponding author. Email: hbudman@uwaterloo.ca
Phone: 519-888-4567 ext. 36980; Fax: 519-746 4979.

mode of operation. In this context, this study compares the flux values obtained in batch and fed batch operations and investigates whether the same structure of the dynamic model is applicable to both.

2. The viable and dead cell concentrations are explicitly modeled. Correlation analysis is used to investigate the dependence of growth and death rates on nutrient and product concentrations. Then, the cell concentrations model is coupled to the metabolites dynamic model to give rise to an overall model that utilizes experimental starting values and predicts for all significant system variables, including viable and dead cell concentrations, independent of subsequent experimental values.

2. MATERIALS AND EXPERIMENTAL METHODS

Murine hybridoma 130-8F producing anti-F-glycoprotein monoclonal antibody (MAb) was provided by Sanofi Pasteur Ltd. (Toronto, Canada) and was propagated in D-MEM medium (Gibco 12100) with 2% FBS (JRH 12107-78P). The medium was supplemented with proline (Sigma P-8449), l-asparagine (Sigma A-4159), and l-aspartic acid (Sigma A-4534). Seed cultures were subcultured on a three-day regime. Seed and batch cultures were grown in 250 mL and 500 mL spinners in a CO_2 incubator (Sanyo IR Sensor, 37 °C, 5.0% CO_2). Batch cultures were maintained for at least 7 days with frequent sampling. To avoid ammonia toxicity, fed-batch cultures were maintained under glutamine-limited conditions and the fed-batch operation was effected by injecting defined amounts of glutamine and glucose solution when its concentration inside the spinner was approaching zero.

Viable and total cell concentration were determined by the Trypan Blue Exclusion test using a haemocytometer. Glucose, lactate, glutamine, and glutamate concentration was quantified using YSI Analyser. Ammonia was measured using a Sigma Ammonia Kit (Sigma 171-B). Total Immunoglobulin titre (MAb concentration) was determined using Enzyme Linked ImmunoSorbent Assay (ELISA) with alkaline phosphatase conjugated goat anti-mouse IgG as the primary reagent. The amino acids in de-proteinated medium were derivatized with OPA (o-phthaldehyde and 3-mercaptopropionic acid in borate buffer) followed with FMOC (9-fluorenylmethylchloroformate in acetonitrile) and assayed using High Performance Liquid Chromatography (Hypersil AA-ODS column).

3. METABOLIC FLUX ANALYSIS

Based on published reports (Bonarius, *et al.,* 1995; Gambhir, *et al.*, 2003; Gao, *et al.,* 2006), a simplified metabolic network shown in Figure 1 is constructed. The figure representing the system under study involves m(=30) metabolites and n(=32) fluxes corresponding to 32 reactions. Mass balances for the intracellular and extracellular metabolites can be represented as follows:

$$\frac{d\boldsymbol{\psi}(t)}{dt} = \mathbf{R}X(t) \qquad (1)$$

where $\boldsymbol{\psi}$ is the vector of intracellular metabolite concentrations and t is the culture time. $\mathbf{R}$ is the vector of uptake/production rate of substrates/metabolites. $X(t)$ is the viable cell concentration and is a function of culture time, t.

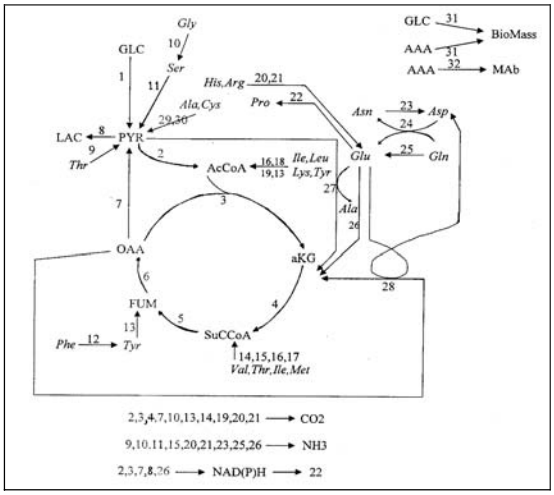

Fig. 1. The simplified metabolic network of Hybridoma cells.

From integration of equation (1) and assuming an average value of R over the integration interval:

$$\int_0^t d\boldsymbol{\psi}(t) = \mathbf{R}\int_0^t dX(t) \qquad (2)$$

$$\Rightarrow \boldsymbol{\psi}_t - \boldsymbol{\psi}_0 = \mathbf{R}(CH_t - CH_0) \qquad (3)$$

CH is referred to as the cumulative volumetric cell hours (Dutton, *et al*., 1998) and can be mathematically expressed as:

$$CH = \int_0^t X(t)dt \qquad (4)$$

Under the assumption of quasi-steady state, the conversion/ production rate, $R(M)$ of a nutrient/metabolite in a biological system is expressed as (Bonarius, *et al.*, 1996):

$$R(M) = \sum_i \alpha_{i,M} j_i \qquad (5)$$

where R is the uptake or production rate of metabolite M (=1…m) and it is calculated from linear regression between measured concentrations of metabolites and volumetric cell hours (CH) based on equation (3). The need for concentration measurements for intracellular metabolites is eliminated by assuming that the system operates under balanced growth conditions and consequently, the corresponding reaction rates (*1* to *6* according to

the notation in Figure 1) are assumed to be equal to 0 (Provost, and Bastin, 2004; Gambhir, *et al.*, 2003). $\alpha_{i,M}$ is the stoichiometric coefficient for metabolite *M* in reaction *i*. $\alpha_{i,M}$ has negative value for substrates that get consumed and is positive for metabolites that are produced. j_i is the intracellular flux for reaction *i*. In matrix notation, equation (5) may be written as:

$$\mathbf{R} = \mathbf{Aj} \tag{6}$$

where **R** is the vector of average uptake or production rates, **j** is the vector of fluxes for all intracellular and extracellular species involved in the system metabolic network (Fig.1) and $\mathbf{A}_{mxn}$ is the matrix of stoichiometric coefficients of the corresponding reaction species.

$$\mathbf{A} = \{\alpha_{iM}\}_{i=1...n, M=1...m} \tag{7}$$

Referring back to system of equations in (6), if only one set of experimental values of **R** is considered, the system will be underdetermined, i.e. less equations than unknowns. However, the system can be made over-determined by considering experimental values of **R** for a number of batches or for measured values of **R** at different times during a fed-batch experiment. For example, if two sets of experimental values of the vector **R** are considered, the augmented system of equations is as follows:

$$\begin{bmatrix} \mathbf{R}_{set1} \\ \vdots \\ \mathbf{R}_{sets} \end{bmatrix}_{smx1} = \begin{bmatrix} \mathbf{A} \\ \vdots \\ \mathbf{A} \end{bmatrix}_{smxn} [\mathbf{j}]_{nx1} \tag{8}$$

$$\mathbf{R}_{\mathrm{mod}} = \mathbf{A}_{\mathrm{mod}}\,\mathbf{j}$$

s: is the number of batches/sections in a fedbatch considered. .

Then, a unique solution for the resulting over-determined system of equations given by (8) can be obtained from the following minimization problem

$$\begin{aligned} &\text{Min } (\mathrm{R_{mod}} - \mathrm{A_{mod}}\mathbf{j})^{\mathrm{T}}(\mathrm{R_{mod}} - \mathrm{A_{mod}}\mathbf{j}) \\ &\text{s.t. } \mathbf{j} \geq \mathbf{0} \end{aligned} \tag{9}$$

The problem in (9) can be solved by a Quadratic Programming (QP) algorithm (Gao, *et al.,* 2006).The result of flux calculation is a metabolic flux network outlining the various biochemical reactions included in the calculations along with an estimate of the steady state rate (i.e., the flux) at which each reaction in figure 1 occurs. Depending on the contribution of each reaction in the network, the smaller flux values that are a negligible portion of the net flux through the system can be eliminated to obtain a reduced metabolic network. The results of this reduction process are given in Section 5.

4. DYNAMIC MODEL

The dynamics involved in a stirred spinner is given by the following macroscopic material balance model:

$$\frac{d\boldsymbol{\xi}(t)}{dt} = \mathbf{K}\mathbf{r}(t) \tag{10}$$

In the equation above, the symbol $\boldsymbol{\xi} = (\xi_1, \xi_2 ... \xi_n)^{\mathrm{T}}$ is the vector of concentrations of extracellular species and is a subset of the vector $\boldsymbol{\psi}$ given by equation (1). $\mathbf{r} = (r_1, r_2 ... r_n)^{\mathrm{T}}$ is the macro-reaction rate vector. **K** is the matrix containing stoichiometric coefficients of the reaction species involved in the elementary macro reactions.

Monod kinetics is assumed for all the reactions according to the general expression:

$$r_i = a_i \left(\prod \frac{Nutrient_i}{Nutrient_i + k_i} \right) X_{v,e} \tag{11}$$

where r_i is the reaction rate for i$^{\mathrm{th}}$ reaction; $\mathrm{Nutrient}_i$ and k_i are the corresponding substrate concentration and half-saturation constant. a_i is the maximum rate at which the reaction can proceed, while $X_{v,e}$ is the experimental viable cell concentration.

As done in previous work (Gao, *et al.,* 2006), the model can be further simplified for calibration purposes by assuming that the half saturation constants k_i's have insignificantly small values in comparison to substrate concentration for major part of the experimental run, i.e. $\mathbf{r}(t) \approx \mathbf{a} X_{v,e}(t)$ and the dynamic model expressed in (10) can thus be stated as:

$$\frac{d\boldsymbol{\xi}(t)}{dt} = \mathbf{K}\mathbf{a} X_{v,e}(t) \tag{12}$$

Additionally, following equation (1) the mass balances for the extracellular metabolites specified by the vector $\boldsymbol{\xi}$ can be expressed as:

$$\frac{d\boldsymbol{\xi}(t)}{dt} = \mathbf{R}_{\boldsymbol{\xi}} X_{v,e}(t) \tag{13}$$

where $\mathbf{R}_{\boldsymbol{\xi}}$ is the conversion rate vector and is a subset of vector **R**. From equations (12) and (13) a system of algebraic equations can be derived as follows:

$$\mathbf{K}\mathbf{a} = \mathbf{R}_{\boldsymbol{\xi}} \tag{14}$$

The system in (14) is generally overdetermined and consequently the **a**-values can be estimated by using again QP to solve the following minimization:

$$\begin{aligned} &\text{Min } (\mathbf{R}_{\boldsymbol{\xi}} - \mathbf{K}\mathbf{a})^{\mathrm{T}}(\mathbf{R}_{\boldsymbol{\xi}} - \mathbf{K}\mathbf{a}) \\ &\text{s.t. } \mathbf{a} \geq \mathbf{0} \end{aligned} \tag{15}$$

The second objective of the study is to model the growth and death of the cells. A general model to describe the viable and dead cells concentrations (as a function of extracellular metabolites) is expressed as follows:

$$\begin{aligned} \frac{1}{X_v}\left(\frac{dX_v}{dt}\right) &= k_g f(\boldsymbol{\xi}) - k_d g(\boldsymbol{\xi}) \\ \frac{1}{X_v}\left(\frac{dX_d}{dt}\right) &= k_d g(\boldsymbol{\xi}) \end{aligned} \tag{16}$$

where X_v and X_d are the viable and dead cell concentration, respectively. Correlation analysis between the experimentally measured terms in the left hand side of equation (16) and different functional forms of nutrient and product concentrations has been used to find these functions. The functional forms $f(\xi)$ and $g(\xi)$ found by correlation analysis are given later in the paper. Finally, the growth and death rate coefficients, k_g and k_d were found by performing the following minimization: Minimize (Sum of squares) =

$$\Sigma\left(X_{v,e}-X_{v,p}\right)^2+\Sigma\left(X_{d,e}-X_{d,p}\right)^2 \qquad (17)$$

where $X_{v,e}$,$X_{v,p}$,$X_{d,e}$ and $X_{d,p}$ are the experimental and predicted values of the viable and dead cell concentrations respectively.

5. RESULTS

For the batch case, the reduced metabolic network was previously obtained by Gao, *et al.*, (2006). To obtain the reduced network for the fed-batch case, exponential phase of one of the fed-batch experimental runs has been subdivided into 10 time intervals defined as time between the instants at which an addition/dilution is made. Post-exponential phase of fed-batch has been defined as decline phase when feeding was stopped. Subsequently, average reaction rates values, as per equation (3), were calculated for each one of these 10 time intervals. Then, the data corresponding to the 10 intervals was simultaneously used to define the over-determined system of equations given by equation (8) and the corresponding fluxes were obtained from the QP solution based on (9).

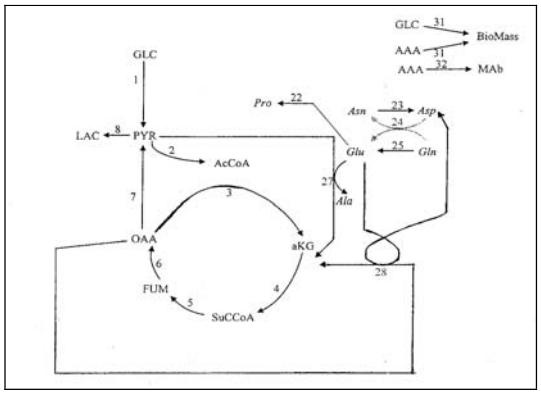

Fig. 2. Reduced Metabolic Network.

Each reaction species in Figure 2 represents a 'flux mode'. Based on the reduced reaction network, the elementary flux modes were computed and in turn, translated into a set of macro-reactions linking/establishing relationships between the various extracellular substrates and products (Provost and Bastin, 2004). The intracellular metabolites were eliminated by simple algebraic manipulation. For example, the reactions:

J1 Glc→2Pyr

J2 Pyr→Lac

Combining J1 and J2 so as to eliminate Pyr:

E1: Glc→2Lac

As a result, 9 elementary macro-reactions were derived (Table 1a) and have been summarized in matrix notation below in Table 1b.

Table 1a Elementary macro reactions

E1	Glc(G)→2Lac
E2	Glc+2Glu(U)→2Ala+2CO_2+2Lac
E3	Glc+2Glu→2Lac+2NH_3+8CO2
E4	Glu→Pro
E5	Asn(S)→Asp+NH_3
E6	Gln(Q)+Asp→Asn+Glu
E7	0.0508Glc+0.0577Gln+0.0133Ala+0.007Arg +0.006Asn+0.0201Asp+0.0004Cys+0.0016Glu +0.0165Gly+0.0033His+0.0084Ile+0.0133Leu +0.0101Lys+0.0033Met+0.0055Phe +0.0081Pro+0.0099Ser+0.008Thr+0.004Tyr +0.0096Val→Biomass
E8	0.0104Gln+0.011Ala+0.005Arg+0.0072Asn +0.0082Asp+0.0005Cys+0.0107Glu +0.0145Gly+0.0035His+0.0054Ile+0.0142Leu +0.0145Lys+0.0028Met+0.0072Phe +0.0148Pro+0.0267Ser+0.0160Thr +0.0085Tyr+0.0189Val→MAb
E9	Gln→Glu+NH_3

Table 1b Matrix of the elementary macro reactions

$$\mathbf{K_{red}}=\begin{array}{c}\\ Glc\\ Gln\\ Lac\\ Glu\\ Asn\\ Asp\\ Ala\\ Pro\\ Biomass\\ MAb\end{array}\begin{bmatrix} r1 & r2 & r3 & r4 & r5 & r6 & r7 & r8 & r9\\ -1 & -1 & -1 & 0 & 0 & 0 & -0.0508 & 0 & 0\\ 0 & 0 & 0 & 0 & 0 & -1 & -0.0577 & -0.0104 & -1\\ 2 & 2 & 2 & 0 & 0 & 0 & 0 & 0 & 0\\ 0 & -2 & -2 & -1 & 0 & 1 & -0.0016 & -0.0107 & 1\\ 0 & 0 & 0 & 0 & -1 & 1 & -0.006 & -0.0072 & 0\\ 0 & 0 & 0 & 0 & 1 & -1 & -0.0201 & -0.0082 & 0\\ 0 & 2 & 0 & 0 & 0 & 0 & -0.0133 & -0.011 & 0\\ 0 & 0 & 0 & 1 & 0 & 0 & -0.0081 & -0.0148 & 0\\ 0 & 0 & 0 & 0 & 0 & 0 & 1 & 0 & 0\\ 0 & 0 & 0 & 0 & 0 & 0 & 0 & 1 & 0 \end{bmatrix}$$

The rows in $\mathbf{K_{red}}$ represent the various metabolites being considered in the model, and the columns represent the number of macro-reactions. It should be noted that unmeasured components such as CO_2 and NH_3 were eliminated in the equations. Since it has been assumed that the reactions shown in Table 1 proceed by Monod kinetics, the reaction rates are expressed as Monod functions of the nutrient concentrations involved in the reaction under consideration. For example, the reaction rate for the reaction (E2): Glc+2Glu→2Ala+2CO_2+2Lac can be expressed as:

$$r_2 = a_2 \frac{Glc}{Glc+k_2}\frac{Glu}{Glu+k_3}X_v \qquad (18)$$

The fundamental macro reactions and their rate expressions are stated in Table 2.

Table 2 Macro reactions and Reaction rates

Reaction	Rate Expression	Parameters
E1	$r_1 = a_1 \frac{G}{G+k_{G1}} X_{v,e}$	a_1, k_{G1}
E2	$r_2 = a_2 \frac{G}{G+k_{G2}} \frac{U}{U+k_{U2}} X_{v,e}$	a_2, k_{G2}, k_U
E3	$r_3 = a_3 \frac{G}{G+k_{G3}} \frac{U}{U+kg_{U3}} X_{v,e}$	a_3, k_{G3}, k_{U3}
E4	$r_4 = a_4 \frac{U}{U+k_{U4}} X_{v,e}$	a_4, k_{U4}
E5	$r_5 = a_5 \frac{S}{S+k_{S5}} X_{v,e}$	a_5, k_{S5}
E6	$r_6 = a_6 \frac{Q}{Q+k_{Q6}} \frac{F}{F+k_{F6}} X_{v,e}$	a_6, k_{Q6}, k_{F6}
E7	$r_7 = a_7 \frac{G}{G+k_{G7}} X_{v,e}$	a_7, k_{G7}
E8	$r_8 = a_8 \frac{Q}{Q+k_{Q8}} X_{v,e}$	a_8, k_{Q8}
E9	$r_9 = a_9 \frac{Q}{Q+k_{Q9}} X_{v,e}$	a_9, k_{Q9}

In light of the above operations, equation 18 reduces to:

$$\frac{d\xi(t)}{dt} = \mathbf{K_{red}} \mathbf{r}(t) \qquad (19)$$

The model calibration is performed on the basis of one batch and one fed-batch experiment, and the estimated a-values are in turn tested for accuracy on an additional batch and fed-batch experiment.

The **a**'s in the reaction rate expressions are calculated separately for exponential and post exponential phase of batch and then for fed-batch operation. It is seen that the **a** coefficients for batch operation necessary to calibrate the model with the data differ from fed-batch operation, and also within one batch the values of **a** for exponential phase of growth are different from the post-exponential phase because of differences in kinetics. The comparison between experiments and predictions are given in figure 3. In these figures experimental cell concentration (also included), was used as input to the dynamic model of metabolites.

To obtain a mathematical model that does not require the experimental data for cell concentration, it was necessary to predict the trends for growth and death of the cells. To be able to do so, it is required to find out what are the influencing factors affecting cell growth and viability. To find the exact dependence, correlation analysis with different Monod expressions of metabolites under study is performed that yields results summarized in Table 3. The terms that did not improve correlation were left out from the overall expression for influencing factor.

Table 3 Results of Correlation Analysis

Expression	Influencing factor	Correlation coefficient highest-value (average-value)
Growth: $\frac{1}{X_v}\left(\frac{dX_v}{dt}\right)$	$\frac{Q}{(Q+0.05)}$	0.93 **(**0.84)
Growth: $\frac{1}{X_v}\left(\frac{dX_v}{dt}\right)$	$\frac{Lac}{(Q+0.43)}$	-0.90 (0.81)
Death: $\frac{1}{X_v}\left(\frac{dX_d}{dt}\right)$	$\frac{Lac}{(Q+0.43)}$	0.92(0.83)

The final step in the formulation of a general model for MAb production was the integration of the dynamic model for extracellular species and the cell concentration model. By combining the two sets of equations meant that instead of using experimental values (as inputs) for model calibration, we will use successively simulated metabolite concentrations and cell concentrations. In short, the systems of equations for the cell culture system under analysis can be stated as follows.

$$\begin{bmatrix} \frac{d\xi}{dt} \\ \frac{dX_v}{dt} \\ \frac{dX_d}{dt} \end{bmatrix} = \begin{bmatrix} Kr(t) \\ k_g\left(\frac{Q}{Q+k_{gQ}}\right) - k_d\left(\frac{Lac}{Q+k_{dQ}}\right) \\ k_d\left(\frac{Lac}{Q+k_{dQ}}\right) \end{bmatrix} X_v \qquad (20)$$

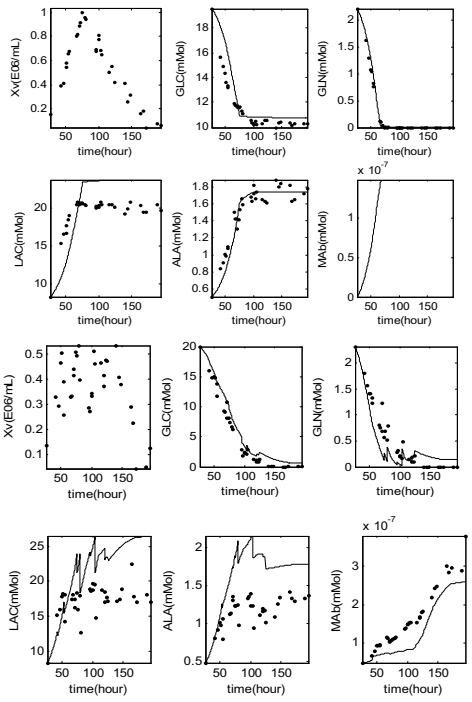

Fig. 3. Comparison of predictions (-) with experimental data for (●) (a) batch and (b) fed-batch. For fed-batch, the various maxima in the graph for X_v correspond to addition of feed to culture.

k_g and k_d for batch mode were 0.04 and 0.001 respectively while for fedbatch these values were 0.04 and 0.0001 respectively. Based on results obtained from model-calibration in (20), a separate set of batch and fed-batch experimental runs was taken to test accuracy of estimated parameters in

predicting future results and have been summarized in Fig. 4.

It was observed from data that while glutamine is not exhausted, the viable cell count was maintained at about $4.5x10^5$ cells/ml and the dead cell count remained relatively low at $1x10^5$ cells/ml. Also, during this period, the death rate k_d was significantly lower for fed-batch as compared to batch mode. The distribution of fluxes during batch and fed-batch operation is shown in Figure 5. Comparing (a) and (b) in Figure 5, it is evident that the ratio of flux 8 (Pyr→Lac) to flux 2 (Pyr→TCA cycle) in batch is 3.2 while in fed-batch it equals 1.8. Moreover, there is a slight increase in flux 1(Glc→Pyr) because there was no Glucose limitation during fed-batch experiment. The fact that during fed batch feeding the death rate k_d was lower whereas the flux of Pyr→TCA-cycle was higher and lactate production was lower seems to indicate that the energy-producing metabolism becomes more efficient as compared to batch. The reason could be a possible metabolic shift with higher emphasis on cellular maintenance rather than growth or metabolite accumulation. There is published evidence to support the above statement (Follstad, *et al*., 1999). Thus, although the set of significant fluxes remains the same in batch and fed-batch operations, the order of dominant fluxes is different.

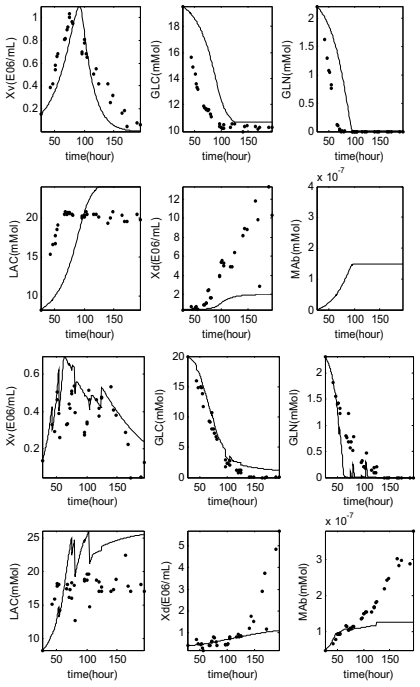

Fig. 4. Predictions(-) for Integrated model vs. Experimental data (●) for (a) batch and (b) fed-batch. Note: Experimental MAb data is unavailable for batch experiment.

6. CONCLUSIONS

Dynamic models for batch and fed-batch operations were derived based on initial metabolic flux analysis. The simplified elementary fluxes and consequent model structure were essentially identical for batch and fed-batch processes. However, differences in reaction rate constants were noted indicating a shift in energy metabolism during fed-batch operation. The results in section 5 imply that the nutrients in fed-batch mode are essentially channelled towards cell-maintenance rather than growth. Future work shall focus on representing death more accurately during the decline phase.

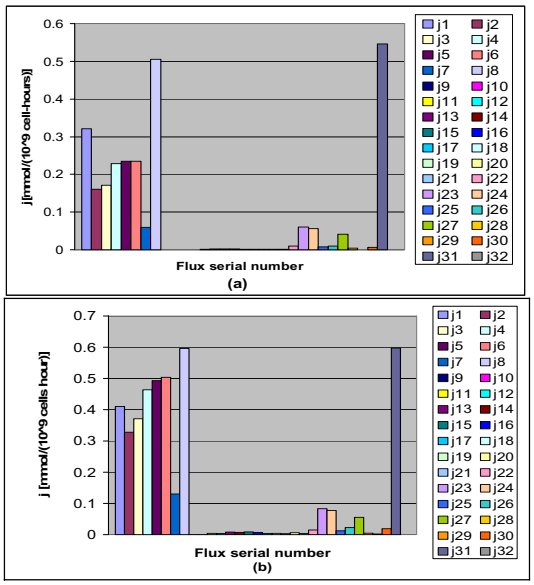

Fig. 5. Distribution of fluxes for (a) batch average and (b) fed-batch average

REFERENCES

Bonarius, H.P.J., V. Hatzimankis, K.P.H. Meesters, C.D.de Gooijer, G. Schmid and J. Tramper (1996). Metabolic Flux Analysis of Hybridoma Cells in Different Culture Media Using Mass Balances. *Biotechnology and Bioengineering*, **50**, pp. 299-318.

Follstad, B.D., R.R. Barcarcel, G. Stephanopolous and D.I.C. Wang, (1999). Metabolic Flux Analysis of Hybridoma Continuous Culture Steady State Multiplicity. *Biotechnology and Bioengineering*, **63,** No.6, pp.675-683

Dutton, R.L., J.M. Scharer and M.Moo-Young (1998). Descriptive parameter evaluation in mammalian cell culture. *Cytotechnology,* **26,** pp 139-152.

Gao, J., V. Gorenflo, J.M. Scharer, and H.M. Budman (2006). Dynamic Metabolic Modeling for the Optimization and Control of Bioprocesses. *To be published*

Gambhir, A., R. Korke, J. Lee, P. Fu, A. Europa and W. Hu (2003). Analysis of Cellular Metabolism of Hybridoma Cells at Distinct Physiological States. *Journal of Bioscience and Bioengineering,* **95**(4), pp. 317-327.

Provost, A. and G. Bastin (2004). Dynamic Metabolic Modelling under the Balanced Growth Condition, *Journal of Process Control* **14,** pp. 717-728.